Analysis of the 13–14 July Gulf Surge Event during the 2004 North American Monsoon Experiment

PETER J. ROGERS AND RICHARD H. JOHNSON

Department of Atmospheric Science, Colorado State University, Fort Collins, Colorado

(Manuscript received 20 April 2006, in final form 29 November 2006)

ABSTRACT

Gulf surges are disturbances that move northward along the Gulf of California (GOC), frequently advecting cool, moist air from the GOC or eastern tropical Pacific Ocean into the deserts of the southwest United States and northwest Mexico during the North American Monsoon (NAM). Little attention has been given to the dynamics of these disturbances because of the lack of reliable high-resolution data across the NAM region. High temporal and spatial observations collected during the 2004 North American Monsoon Experiment are used to investigate the structure and dynamical mechanisms of a significant gulf surge on 13–14 July 2004. Integrated Sounding Systems deployed along the east coast of the GOC and an enhanced network of rawinsonde sites across the NAM region are used in this study. Observations show that the 13–14 July gulf surge occurred in two primary stages. The first stage was preceded by anomalous low-level warming along the northern GOC on 13 July. Sharp cooling, moistening, and increased low-level south-southeasterly flow followed over a 12–18-h period. Over the northern gulf, the wind reached ~20 m s^{-1} at 750 m AGL. Then there was a brief respite followed by the second stage—a similar, but deeper acceleration of the southerly flow associated with the passage of Tropical Storm (TS) Blas on 14 July. The initial surge disturbance traversed the GOC at a speed of ~17–25 m s^{-1} and resulted in a deepening of the mixed layer along the northern gulf. Dramatic surface pressure rises also accompanied the surge. The weight of the evidence suggests that the first stage of the overall surge itself consisted of two parts. The initial part resembled borelike disturbances initiated by convective downdrafts impinging on the low-level stable layer over the region. The secondary part was characteristic of a Kelvin wave–type disturbance, as evident in the deeper layer of sharp cooling and strong wind that ensued. Another possible explanation for the first part is that the leading edge of this Kelvin wave steepened nonlinearly into a borelike disturbance. The second stage of the surge was associated with the increased circulation around TS Blas.

1. Introduction

The North American Monsoon (NAM) is an atmospheric circulation phenomenon characterized by an increase in convective activity and precipitation, beginning in early July and continuing through mid-September across northwest Mexico and the southwest United States (Bryson and Lowry 1955; Douglas et al. 1993; Adams and Comrie 1997). Monsoon onset was originally attributed to the westward extension of the southeast United States subtropical high (Jurwitz 1953; Bryson and Lowry 1955; Sellers and Hill 1974), resulting in a midtropospheric wind shift from dry westerlies to moist southeasterlies. However, the source of low-level moisture associated with monsoon onset along the Gulf of California (GOC) and into Arizona remained unclear (Reitan 1957; Rasmusson 1967). A partial resolution of this issue came about through the studies of Hales (1972) and Brenner (1974), who introduced the moisture "gulf" surge (hereafter gulf surge) as a mechanism for transporting low-level cool, moist air northward along the GOC during the NAM.

Hales (1972) suggested that a natural channel exists along the GOC [Baja peninsular ranges to the west and Sierra Madre Occidental (SMO) to the east] for gulf surge propagation (Fig. 1). Because of decreased frictional effects over water, gulf surges are strongest over the GOC and continue most forcefully up the Colorado River basin upon reaching the northernmost extent of the GOC (Hales 1972; Brenner 1974). Hales (1972) found that a gulf surge on 1–2 September 1970 tra-

Corresponding author address: Peter J. Rogers, Department of Atmospheric Science, Colorado State University, Fort Collins, CO 80523.
E-mail: peter.rogers@noaa.gov

DOI: 10.1175/MWR3450.1

versed the entire length of the gulf at a speed of ~15 m s^{-1}. Simulations of gulf surges by Stensrud et al. (1997) found speeds over a wide range of 10–23 m s^{-1}.

Several common characteristics of gulf surges have been well-documented (Hales 1972; Brenner 1974), and summarized by Fuller and Stensrud (2000): 1) gulf surge onset is accompanied by a significant drop in surface temperature, increases in sea level pressure and surface dewpoint temperature (relative humidity), a surface wind shift with an increased southerly component, and increased low-level cloudiness; 2) gulf surge–related cooling and moistening are greatest just above the surface and decrease with height; 3) gulf surges are strongest at their onset, but decrease in intensity once having fanned out over the low deserts of Arizona; and 4) deep gulf surges can potentially increase convective development across much of Arizona. Douglas and Leal (2003) further elucidated the kinematic and thermodynamic characteristics of gulf surges in a sounding composite study.

Hales (1972) and Brenner (1974) also discovered a connection between large cloud masses over the central and/or southern GOC and subsequent surges of moisture, implying a disturbance in the low-level pressure balance along the GOC. The amplification of the along-gulf pressure gradient provides the impetus necessary to transport moisture northward. Several studies have since linked the development of these large cloud masses with westward-moving hurricanes, tropical storms, or midtropospheric easterly waves (Stensrud et al. 1997; Fuller and Stensrud 2000; Douglas and Leal 2003). Others have suggested connections with upper-tropospheric inverted troughs (Pytlak et al. 2005) or mesoscale convective systems (MCSs) that develop along the SMO and GOC coastal plain (Adams and Comrie 1997).

The dynamical mechanisms by which gulf surges propagate northward along the GOC have received little attention in the literature, especially from an observational standpoint. Most likely this is a consequence of little reliable high-resolution data across the NAM region except for brief periods during the Southwest Area Monsoon Project (SWAMP) in 1990 (Douglas 1995) and 1993 (Douglas and Li 1996). Zehnder (2004) investigated four possible gulf surge dynamical mechanisms: gravity currents, ageostrophic isallobaric flow, Rossby edge waves, and barrier Kelvin waves. He found that Rossby or Kelvin wave dynamics may be an explanation for this phenomenon, but the results were inconclusive.

Zehnder (2004) noted that detailed observations are needed to confirm or refute various theories of the dynamics of gulf surges. Therefore, the primary objective of this study is to use high-resolution data collected during the 2004 North American Monsoon Experiment (NAME) to describe in unprecedented detail the structure of a significant gulf surge event on 13–14 July 2004, and attempt to understand its dynamical mechanisms.

2. Data and methods

a. NAME structure and gulf surge identification

The NAME extended observing period (EOP) was conducted from 1 June to 30 September 2004, although many instrumentation platforms were only in operation from 1 July to 15 August. During this latter period, there were nine intensive observing periods (IOPs) involving 18 IOP days. IOPs were generally accompanied by an increased frequency of rawinsonde launches from the sounding network (Fig. 1) and National Oceanic and Atmospheric Administration (NOAA) WP-3D aircraft flights in the vicinity of the GOC.

The gulf surge investigated in this study occurred primarily on 13–14 July during IOP 2 (Higgins et al. 2006). To capture pre- and postsurge conditions, the period of interest examined for this event was 0000 UTC 12 July–0000 UTC 15 July. Several other surges were observed from 1 July to 15 August, but the 13–14 July case was one of only two major events during the NAME, the other occurring on 22–24 July.

b. Integrated Sounding System

Maintained by the National Center for Atmospheric Research (NCAR), three Integrated Sounding Systems [ISSs; located at Puerto Peñasco and Bahia Kino in Sonora (SON), and Los Mochis in Sinaloa (SIN), Mexico] were deployed from 7 July to 15 August (Fig. 1). The ISSs consisted of 1) a global positioning system balloon-borne atmospheric rawinsonde system, which measured pressure, temperature, relative humidity, and wind speed/direction at 1-s resolution; 2) a 915-MHz Doppler clear-air wind profiling radar (hereafter profiler), which measured wind speed and direction (~100-m vertical resolution) up to several kilometers AGL at half-hour intervals; 3) an enhanced surface observing station, which measured surface pressure, temperature, relative humidity, wind speed/direction, radiation, and precipitation at 1-min resolution; and 4) a Radio Acoustic Sounding System (RASS), which measured vertical profiles of virtual temperature at half-hour intervals. Because of the proximity of the ISS sites at Puerto Peñasco and Bahia Kino to the local populace and the unpleasant sound that the RASS emits, operators shut down the system at night (approximately 2200–0800 LT) at these sites. Unfortunately, initial gulf

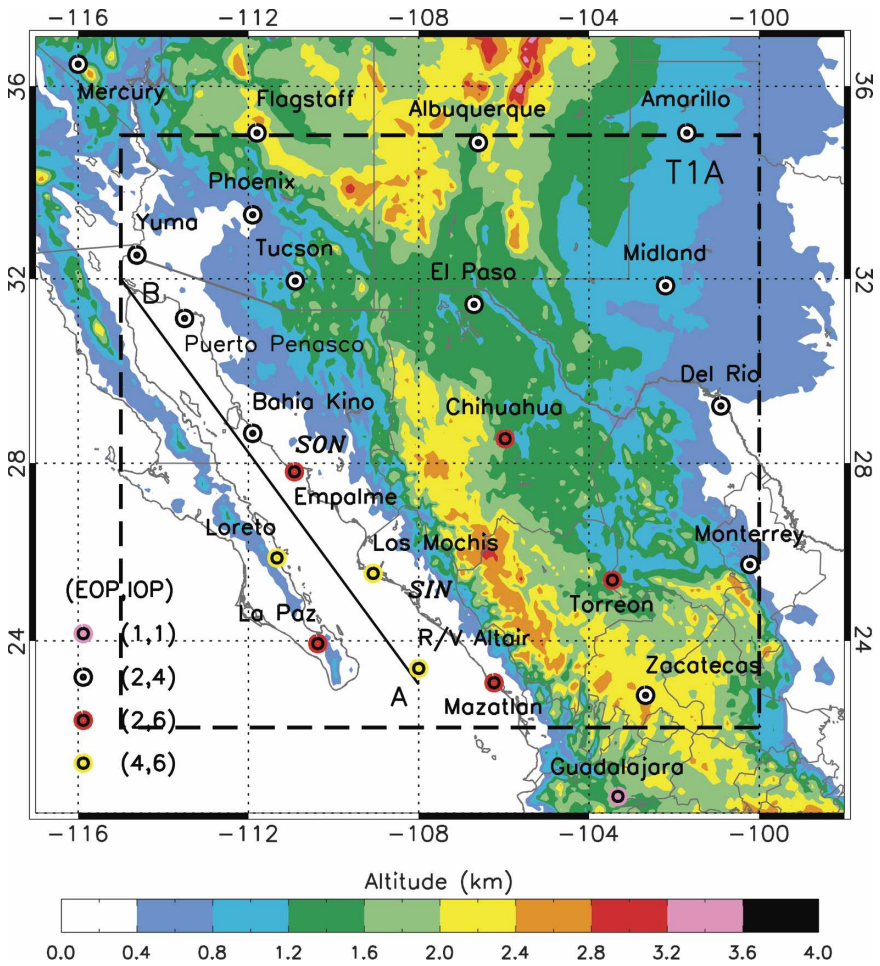

FIG. 1. 2004 NAME EOP rawinsonde sites. The site symbol refers to the number of rawinsonde launches per day during the EOP and nine IOPs. The heavy dashed curve outlines the T1A domain. The solid curve (A–B) through the axis of the GOC identifies the locations of the vertical cross sections shown in Fig. 9. Colored contours represent elevation above sea level (m).

surge passage occurred in the early morning and was not observed by the RASS along the northern GOC. Therefore, RASS data were not used in this study.

ISS sounding data were run through the NCAR-developed Atmospheric Sounding Processing Environment quality control program, which smoothed the profiles and removed suspicious data points. Additional quality control was later conducted that included visual checks and profile comparisons to check for major discrepancies (W. Brown 2004, personal communication). The NCAR Improved Moments Algorithm (NIMA) quality control program was used to correct bad or questionable profiler data. In addition, only those data with confidence values greater than 0.5, as calculated using the NCAR Winds and Confidence Algorithm (NWCA), were considered reliable (W. Brown 2004, personal communication). In constructing wind profiler plots, surface data were added from the surface meteorological stations since the first profiler range gate was ~120–180 m AGL. The quality of the data collected at the ISS surface stations was excellent, requiring no significant quality control effort.

c. *NAME rawinsondes and observational gridded analyses*

An extensive rawinsonde network (Fig. 1) was operational during the NAME EOP. In the region 15°–40°N, 90°–120°W, the National Weather Service (NWS) supported 23 sites, 10 of which launched four rawinsondes per day during the IOPs, while the Servicio Meteorológico Nacional [(SMN) Mexican Weather Service] supported 13 sites, 5 (2) of which launched 6 (4) rawinsondes per day during the IOPs. Other sites with high temporal frequency rawinsonde launches

with varying schedules included the R/V *Altair* at the mouth of the GOC (23.5°N, 108°W); Loreto, Baja California Sur; and Yuma, Arizona.

All NAME sounding data, including those from the ISS sites were processed through additional quality control procedures that mimicked those used during the Tropical Ocean Global Atmosphere Coupled Ocean–Atmosphere Response Experiment (Loehrer et al. 1996). These procedures included the computation of statistical means and standard deviations to check gross limits, objectively flagging data as questionable or bad, linear interpolation over missing data gaps, and visual inspection.

The quality-controlled data collected from all rawinsonde sites were objectively analyzed using a multiquadric interpolation (Nuss and Titley 1994) onto a 1° × 1° grid over 15°–40°N, 90°–120°W [tier-2 array (T2A)] 2 times per day (0000 and 12000 UTC), and over 22°–35°N, 100°–115°W [tier-1 array (T1A); Fig. 1] 4 times per day (0000, 0600, 1200, and 1800 UTC) with 25-hPa vertical resolution (surface, 1000–50 hPa). In addition, profiler data from the ISS sites were included in the gridded analyses at those times when rawinsonde winds were unavailable. The National Centers for Environmental Prediction (NCEP)–NCAR reanalyses data (Kalnay et al. 1996) were used only over data-sparse regions of the east Pacific Ocean and Caribbean Sea to assist the analysis; however, the NCEP–NCAR data do not affect results over the core (GOC) region of the analysis (Johnson et al. 2007).

d. Additional datasets

Surface pressure data from numerous sites that report hourly observations using the standard World Meteorological Organization (WMO) aviation routine weather report (METAR) format were used in conjunction with ISS surface data to investigate surface pressure patterns associated with the surge event. Because of the lack of observations over Baja California, data were used from the SMN 10-min automated surface observing network to improve coverage over the peninsula. However, the overall quality of surface pressure data at the SMN sites (both WMO and automated) were quite poor and included unrealistic high-frequency noise. An objective scheme was developed to remove the most obvious surface pressure errors, which was applied to all sites. Values greater than four standard deviations from the site's 7 July–14 August mean were set to missing. Missing data gaps less than or equal to 6 h were then filled by linear interpolation.

In addition, *Geostationary Operational Environmental Satellite-10* (*GOES-10*) infrared (IR) images centered about the core monsoon region were obtained from the NAME field catalog (available online at http://catalog.eol.ucar.edu/name/) to determine areas of relative cloudiness and convective activity associated with gulf surge initiation, propagation, and passage. No NAME pilot balloon, aircraft, or radar data were used in this study.

3. Large-scale environment

a. Synoptic conditions

Figure 2 highlights the T2A 700- and 200-hPa heights and wind vectors at 1200 UTC 12–14 July. At 700 hPa (Fig. 2a), two significant features are evident: a subtropical high over the southern United States and Tropical Storm (TS) Blas moving northwestward across the southwestern corner of the domain. At 200 hPa (Fig. 2b), an upper-tropospheric inverted trough (evident on 12 July as a closed low over northern Mexico) propagated to the south and west of the upper-level anticyclone over the southern United States. As the trough propagated west-northwestward, it weakened so that by 13 July it was no longer discernable (Fig. 2b). Water vapor imagery examined by Pytlak et al. (2005) suggests that the trough dissipated along the international border on 13 July.

The general location, movement, and timing of TS Blas are consistent with the interpretations of Fuller and Stensrud (2000) and Douglas and Leal (2003), who have related gulf surge initiation with easterly wave or tropical cyclone passage south of the GOC. Higgins and Shi (2005) have also shown that surges associated with tropical cyclones are often deeper and more intense than those that are not linked to tropical cyclone propagation. The combination of TS Blas and the subtropical high generated strong southeasterly wind south of the mouth of the GOC on 13 July and over much of the GOC by 14 July at 700 hPa.

b. Convective conditions

Figure 3 shows *GOES-10* IR satellite images centered on the core NAM region every 6 h from approximately 1800 UTC 12 July to approximately 0000 UTC 14 July. At 1754 UTC (~1200 LT) 12 July (Fig. 3a), a large convective cluster extended northward from TS Blas's center of circulation south of the mouth of the GOC. By 2345 UTC 12 July (Fig. 3b), a thunderstorm complex developed over northern Sonora and southeast Arizona and isolated convective storms formed farther south along the SMO. Upper-level divergence associated with the inverted trough may have aided in the convective development along the SMO (Pytlak et al. 2005).

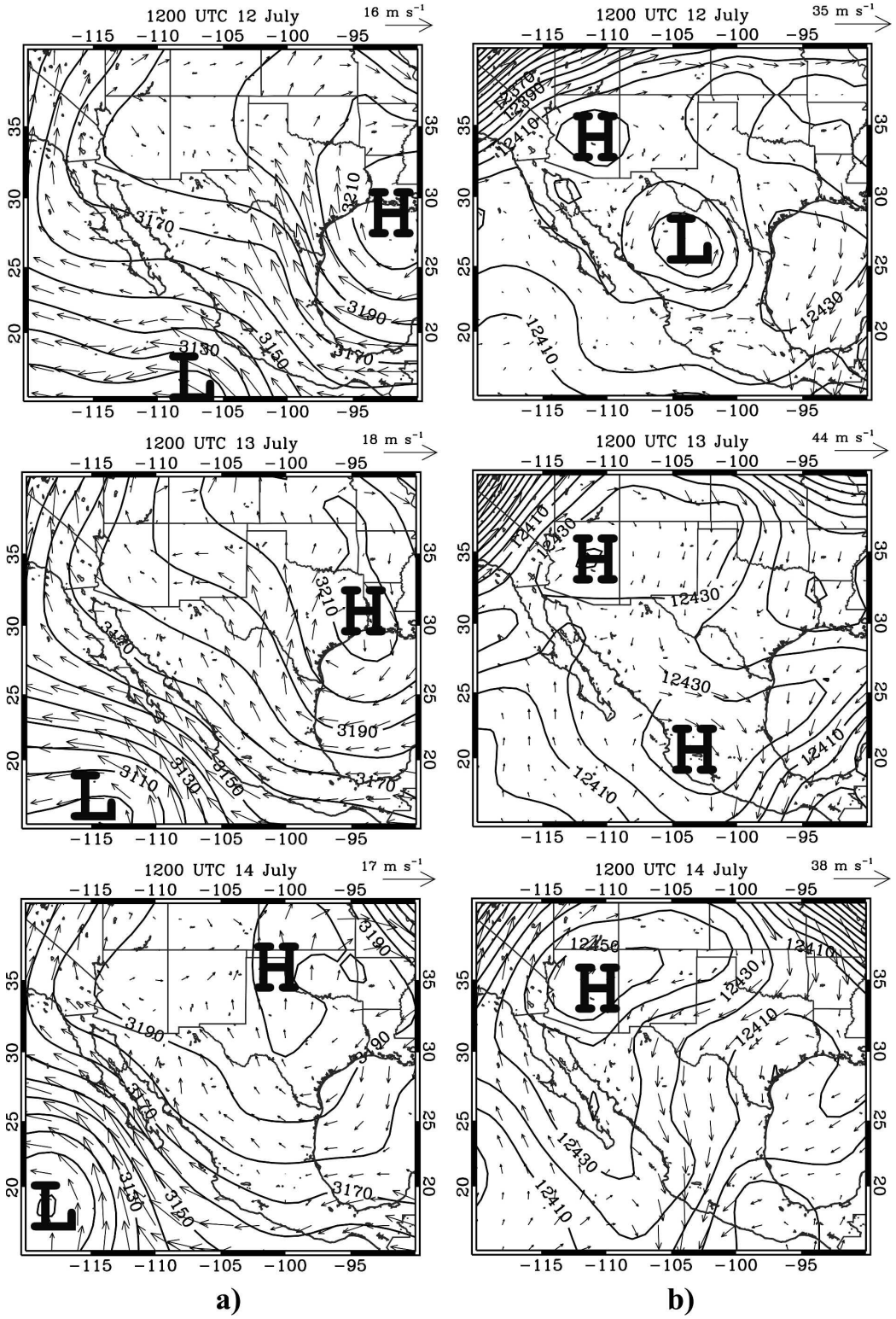

FIG. 2. T2A (a) 700- and (b) 200-hPa heights (10-m intervals) and wind vectors ($m\ s^{-1}$) at 1200 UTC from 12 Jul to 14 Jul 2004. High and low heights are labeled H and L, respectively.

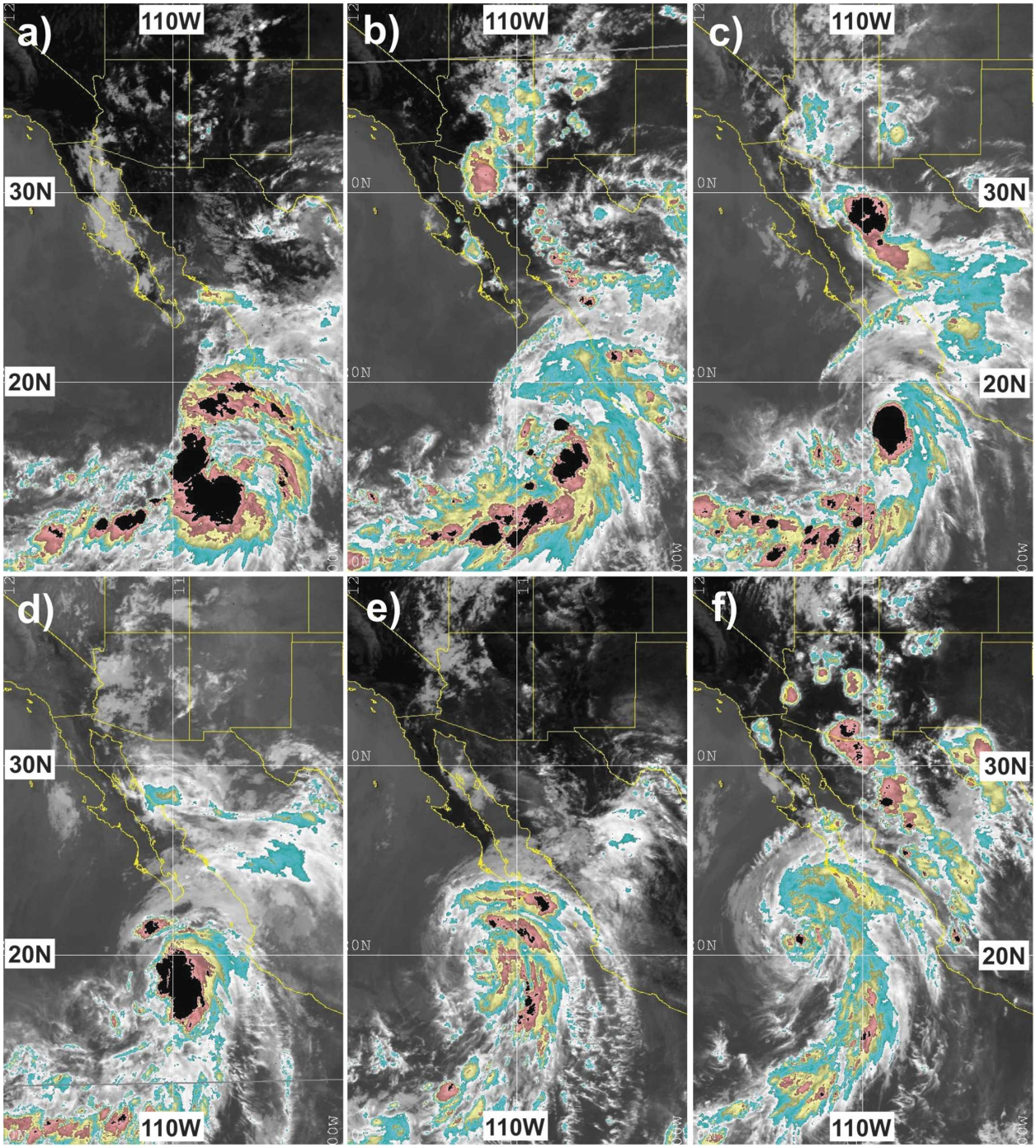

FIG. 3. Infrared *GOES-10* satellite imagery over the core NAM domain at (a) 1754 UTC 12 Jul, (b) 2345 UTC 12 Jul, (c) 0554 UTC 13 Jul, (d) 1154 UTC 13 Jul, (e) 1754 UTC 13 Jul, and (f) 2354 UTC 13 Jul 2004. Colder cloud tops (°C) are shaded darker.

Six hours later (0554 UTC 13 July; Fig. 3c) TS Blas was farther north and its outer rainbands penetrated the southern GOC and Baja Peninsula. The convective cells over the SMO merged with the thunderstorm complex over northern Sonora to form an impressive MCS over the central GOC coastal plain. The MCS quickly dissipated over the central gulf by 1154 UTC (~0600 LT) 13 July (Fig. 3d) as TS Blas continued along its northwestward trajectory.

By the afternoon (1754 UTC) of 13 July (Fig. 3e), convective activity over the northern and central GOC was suppressed, although TS Blas's circulation center

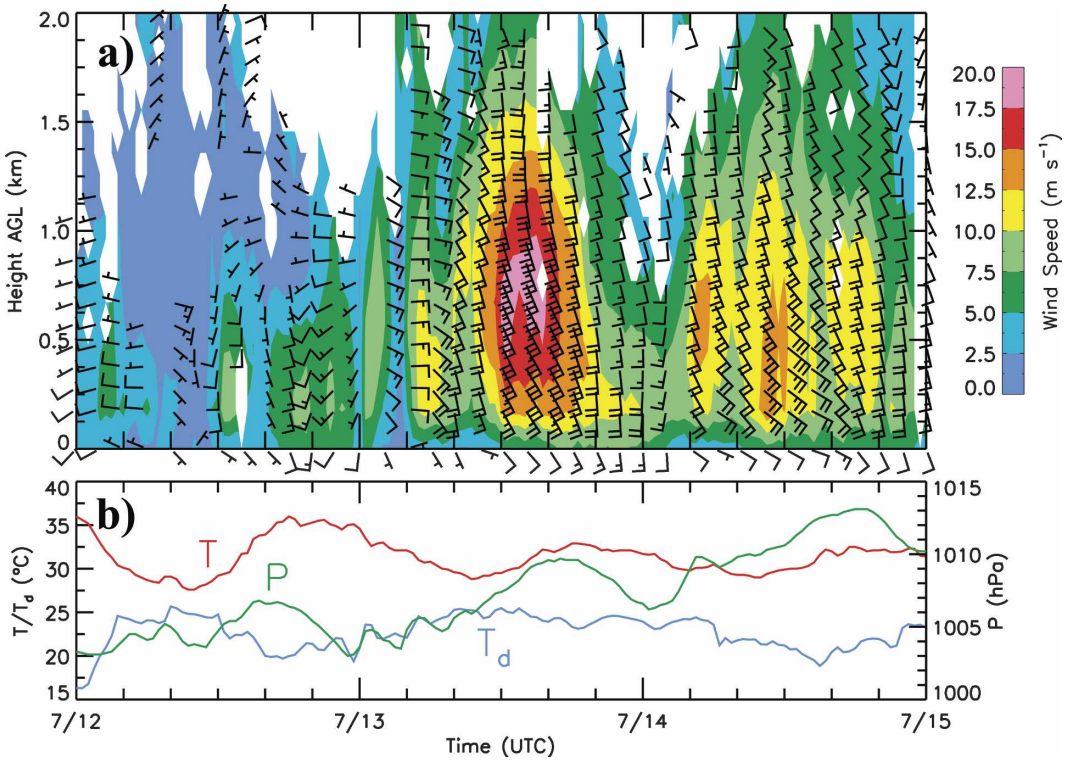

FIG. 4. Puerto Peñasco (a) wind profiler and (b) surface data from 0000 UTC 12 Jul to 0000 UTC 15 Jul. In (a), wind speed (m s^{-1}, colored contours) is plotted every half-hour and wind barbs every 2 h. One full barb equals 5 m s^{-1}. Only those times and heights are plotted where NIMA/NWCA confidence values are greater than or equal to 0.5. In (b), surface temperature (°C, red), dewpoint temperature (°C, blue), and pressure (hPa, green) are averaged over and plotted every half-hour.

was now clearly visible to the southwest of Baja California. At 2354 UTC 13 July (Fig. 3f), the rainbands from TS Blas spread over much of the central and southern GOC, while a large MCS began to develop along the international border between Arizona and Sonora. The development of this MCS was potentially aided by the northward transport of moisture by the gulf surge (McCollum et al. 1995) and the midtropospheric synoptic regime (Higgins et al. 2004).

4. Gulf surge structure

a. Vertical structure as observed by ISS profilers

Heretofore, Douglas and Leal (2003) have conducted the most comprehensive analysis of gulf surge vertical structure and evolution using 12-h rawinsonde data at Empalme (in Sonora) over nine years. However, the NAME ISSs provide a much higher vertical and temporal resolution of this phenomenon (~100 m, half-hour). In this section wind profiler data, along with the surface observations, are presented at the ISS sites for the period 12–14 July.

Gulf surge onset at Puerto Peñasco (Fig. 4a) occurred at approximately 1000 UTC 13 July, evident in strong south-southeast winds up to 12.5 m s^{-1} centered near 750 m AGL extending from ~250 m to 1.25 km AGL. The surge quickly intensified and deepened, so that by 1400 UTC, maximum wind speeds approached 20 m s^{-1} near 750 m and the surge extended vertically to near 2.0 km. The strength and location of the peak wind at Puerto Peñasco are in good agreement with NOAA WP-3D wind measurements obtained from a sawtooth flight pattern over the northern GOC on the afternoon of 13 July (not shown) and are also in good agreement with previous SWAMP flights (Douglas 1995; Stensrud et al. 1997). The significant low-level flow perturbations at Puerto Peñasco prior to surge onset on 13 July will be discussed in section 5.

The surface wind did not respond as dramatically to the surge onset as did the flow aloft, but eventually increased to 5–7.5 m s^{-1} from the south-southeast at 1200 UTC, and at times nearly 10 m s^{-1} after 1600 UTC. The surge signal aloft weakened by 0000 UTC 14 July. In addition, strong southeasterly flow occurred during most of 14 July below ~1.25 km with maximum

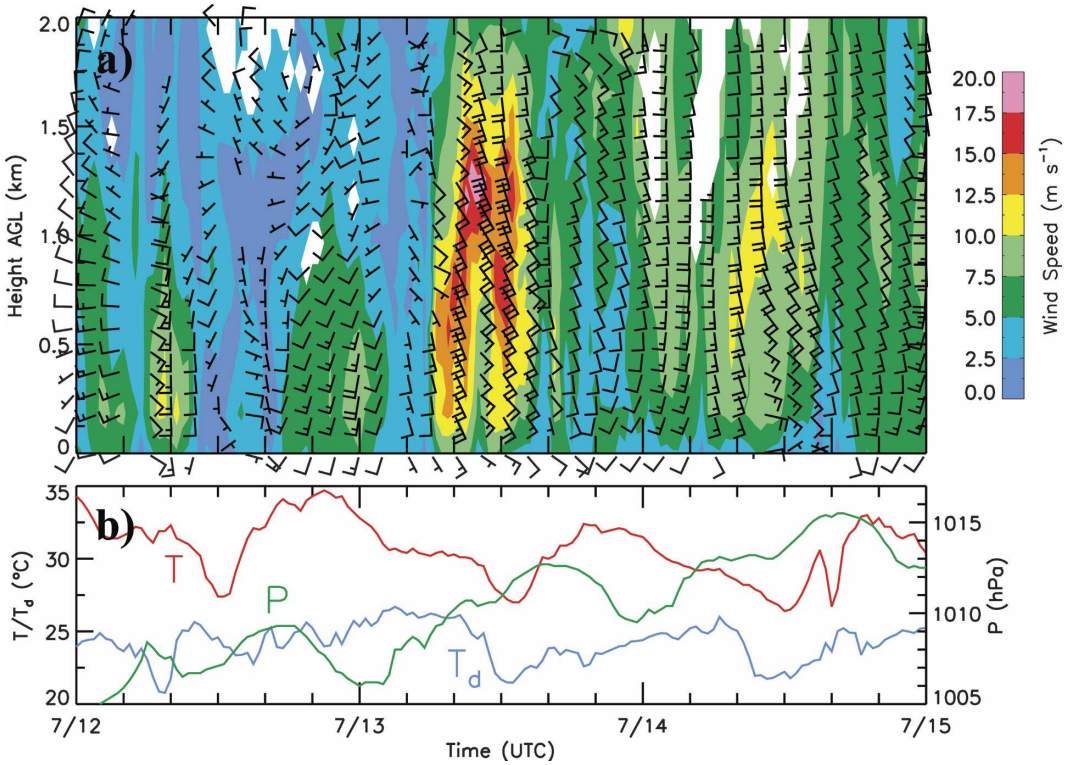

FIG. 5. Same as in Fig. 4, but at Bahia Kino.

speeds as high as 16 m s^{-1}. This pattern does not appear to be a continuation of the prior day's gulf surge. Rather, Figs. 2a and 3 suggest it is due to the northwest propagation of TS Blas.

The most notable surface feature during the surge passage was a steady pressure rise (following two brief rises early on 13 July associated with convective outflows, to be discussed later) that began at ~0800 UTC (Fig. 4b) and continued for 36 h resulting in an overall pressure increase of ~8 hPa.[1] During and following the surge event, daily afternoon maximum temperatures were reduced, although changes in the dewpoint temperature were minor. This behavior contrasts with the dramatic dewpoint increase from 0000 to 1700 UTC 13 July (~12°C) that occurred at Yuma accompanying this surge. A sudden rise in the dewpoint has often been used to identify surge arrival in Arizona (Stensrud et al. 1997; Fuller and Stensrud 2000). The different behavior at Puerto Peñasco and Yuma can be attributed to the different ambient (presurge) conditions between the moist GOC coastline and the interior deserts of Arizona.

Gulf surge onset farther south at Bahia Kino appeared abruptly at 0600 UTC 13 July (Fig. 5a). There was an acceleration of the low-level flow with the peak wind approaching 20 m s^{-1} from the south-southeast near 1.25 km AGL by 1000 UTC. Overall, the altitude of the wind maximum was ~500 m higher than at Puerto Peñasco. Southeasterly surface flow increased to 7.5 m s^{-1} shortly after 0600 UTC and remained at or above 5.0 m s^{-1} through much of the day. Similar to Puerto Peñasco, the surge quickly weakened and appeared disconnected from the strong south-southeasterly flow on 14 July associated with TS Blas. A pressure rise at the surface of ~9 hPa occurred that began at 0200 UTC and continued for 40 h. Surface temperature and moisture changes qualitatively mimicked those at Puerto Peñasco (Fig. 5b).

The character of the surge at Los Mochis (Fig. 6a) was different from its appearance at Puerto Peñasco and Bahia Kino. The period of increased south-southeasterly flow extending to 2 km from approximately 0000 to 1200 UTC 13 July is the gulf surge signal at Los Mochis. Maximum winds reached 12.5 m s^{-1} between 800 m and 1.5 km AGL near 1000 UTC. The short (~2 h), strong wind burst from the southeast be-

[1] The surface traces presented in Figs. 4b, 5b, and 6b are raw observations and therefore include atmospheric tidal effects, unlike Fig. 11, which shows anomalies. Surge-related surface changes are best depicted in Fig. 11.

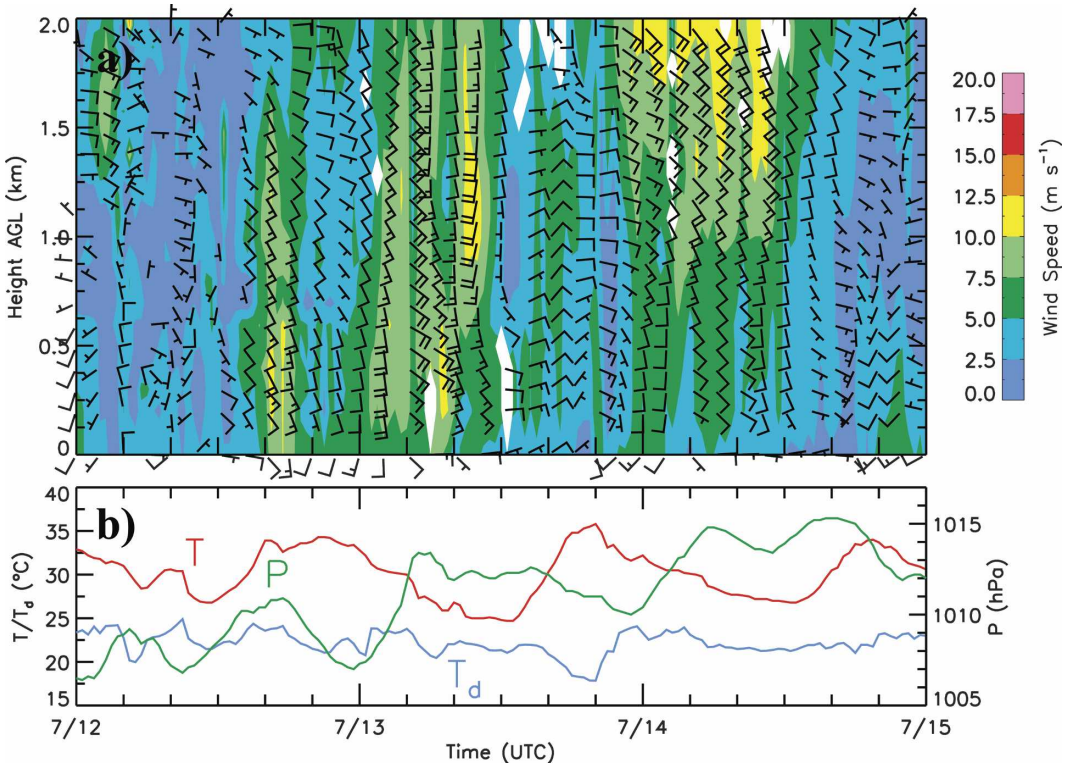

FIG. 6. Same as in Figs. 4 and 5, but at Los Mochis.

ginning at 1600 UTC 12 July is not part of the gulf surge because it is followed by a 6-h lull in the flow, and can be traced back to a strong convective outflow from a nearby thunderstorm cluster using visible satellite imagery (not shown). This outflow is ill defined from the surface parameters in Fig. 6b because half-hour averaging was applied to the data. The profiler gulf surge signatures at Puerto Peñasco and Bahia Kino quickly amplified and deepened, as did the Los Mochis signal after 0000 UTC 13 July. In summary, the profiler data show the surge to be weaker over the southern GOC although its onset was earlier there than at the northernmost ISS sites.

NOAA WP-3D aircraft measurements during a flight along the GOC suggested that the height of maximum southerly wind associated with a gulf surge examined during SWAMP 1990 increased from north to south (Stensrud et al. 1997). Although the flow is weaker along the southern gulf compared with the north on 13 July, a similar wind structure generally emerges from the results of this study (Figs. 4a, 5a, and 6a). The differences in the strength of the flow from north to south may in part be explained by the fact that the timing of the surge in the north is coincident with the GOC nocturnal low-level jet (LLJ; Douglas 1995; Douglas et al. 1998), leading to an amplification of the flow. This LLJ was present ~75% of the mornings at Yuma during SWAMP 1990 with the strongest wind located between 300 and 600 m and maximum speeds reaching 20 m s^{-1} (Douglas 1995) peaking at 0100 LT along the GOC east coast (Douglas et al. 1998). These results indicate that the gulf surge traversed the length of the GOC and first passed Los Mochis around 0000 UTC 13 July. Surge structure varied from south to north, with the flow being stronger and shallower in the north, consistent with the WP-3D aircraft observations on 13 July (Higgins et al. 2006) and previous studies (Stensrud et al. 1997).

The time series of surface observations at Los Mochis (Fig. 6b) indicate a substantial increase in the surface pressure (~8 hPa) beginning near 0000 UTC 13 July and continuing through 1600 UTC 14 July. Following surge passage, there was no distinct change in the normal diurnal cycle of temperature and dewpoint temperature.

Given the continuity of surface pressure increases at the ISS sites, maps of surface pressure anomalies were constructed using data from the WMO METAR, ISS, and SMN automated sites to track the regional impacts of the surge on the surface pressure field (Fig. 7). Data shown are surface pressure anomalies (from 7 July to 14 August means) every 6 h interpolated onto a regular 0.5° × 0.5° grid over the core NAM region. Anomalies

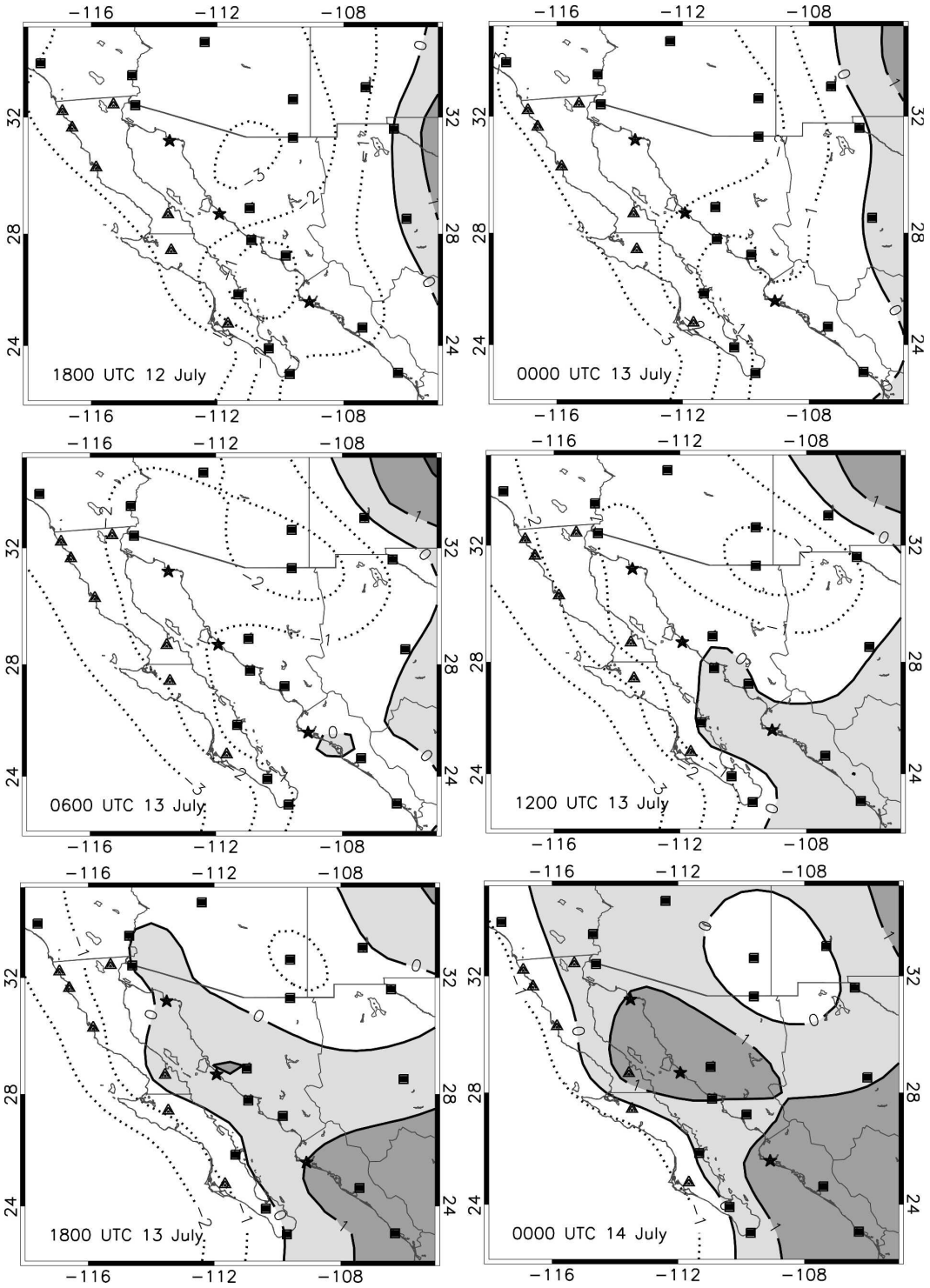

FIG. 7. The 25-h running mean surface pressure anomaly isobars (hPa) from 1800 UTC 12 Jul to 0000 UTC 14 Jul 2004. Anomalies are calculated using 7 Jul–14 Aug means. Dotted contours are negative and shaded contours are positive. Contours over the eastern Pacific Ocean have been omitted because of the lack of observational pressure data in this region. Squares denote NWS or SMN WMO sites, triangles denote SMN automated sites, and stars denote ISS sites.

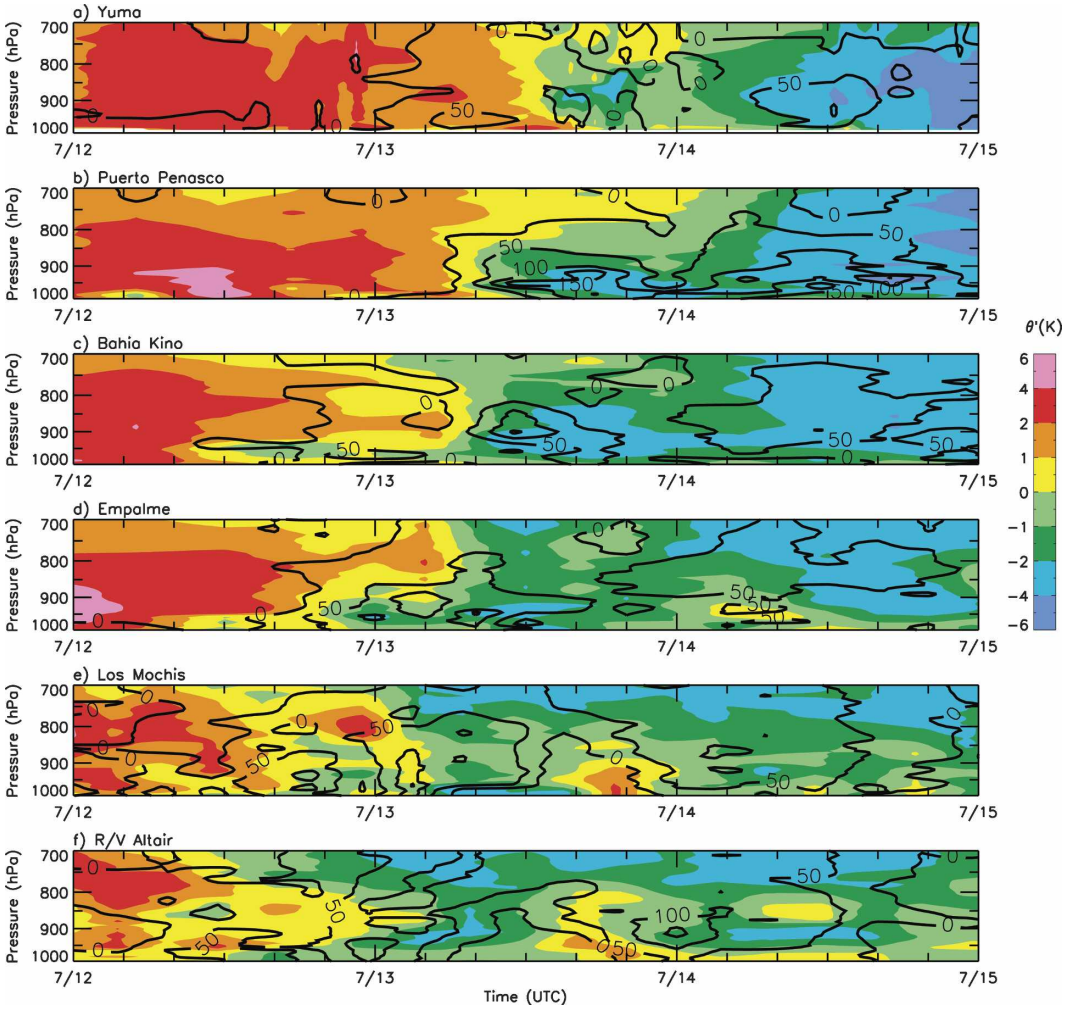

FIG. 8. Half-hour interpolated rawinsonde potential temperature and moisture flux anomalies at (a) Yuma, (b) Puerto Peñasco, (c) Bahia Kino, (d) Empalme, (e) Los Mochis, and (f) R/V *Altair* from 0000 UTC 12 Jul to 0000 UTC 15 Jul 2004. Anomalies are calculated using 5 Jul–15 Aug means. Colored contours represent potential temperature anomalies (K). Black curves represent positive moisture flux anomalies in 50 m g s^{-1} kg^{-1} intervals.

were used because some sites reported sea level pressure and others reported station pressure. Twenty-five-hour running means were used to smooth the data and remove the diurnal and semidiurnal tides.

At 1800 UTC 12 July (Fig. 7), the GOC region was dominated by negative anomalies. By 1800 UTC 13 July, positive anomalies replaced negative values along much of the GOC and its coastal plain. This behavior agrees qualitatively well with a similar surge-related surface pressure analysis conducted by Douglas and Leal (2003) using 9 yr of NCEP–NCAR reanalysis data. By 0000 UTC 14 July, surface pressure anomalies greater than +1 hPa were located over the northern GOC. This maximum strengthened significantly over the following 24 h (not shown) so that by 0000 UTC 15 July, areas over the Sonoran Desert had surface pressure anomalies of +4 hPa or more. These continued pressure rises are likely related to the propagation of TS Blas (Figs. 2a and 3).

b. *Vertical structure as observed by rawinsondes*

To further explore the properties of the gulf surge along the GOC, time series were created from the 4- or 6-hourly sounding data linearly interpolated to half-hour intervals. Potential temperature and moisture flux (meridional wind multiplied by mixing ratio) anomalies were computed from 1000 to 700 hPa at six sites (Yuma, Puerto Peñasco, Bahia Kino, Empalme, Los Mochis, and R/V *Altair*) for the period 0000 UTC 12 July–0000 UTC 15 July (Fig. 8). To calculate the anomalies, average values determined for each half-hour of the day over the period 5 July–15 August were subtracted from

the corresponding individual times. In doing this, the diurnal tidal signals were removed in a mean sense. Interpolation was conducted over data points flagged as bad or questionable from the quality control procedure and a 1–2–1 filter was applied in the vertical to smooth high-frequency noise.

Warming throughout the column was observed at each site prior to gulf surge onset (Figs. 8a–f). This warming was especially strong near the surface and along the northern GOC (+2 to +6 K). Warming signatures at Los Mochis (Fig. 8e) and the R/V *Altair* (Fig. 8f) were less well defined and generally weaker. The warming pattern agrees well with the composite results of Douglas and Leal (2003). They show anomalous warming of +2.5°C one day prior to gulf surge onset peaking around 950 hPa at Empalme.

Gulf surge onset occurred abruptly during the early morning on 13 July, and is readily identified by the large maxima of positive moisture flux and associated cooling from Empalme north to Yuma. The changes were largest below 800 hPa, in agreement with Douglas and Leal (2003), and lasted for several hours. The greatest cooling (−2 to −4 K) and positive moisture flux (>+150 m g s^{-1} kg^{-1}) occurred at Puerto Peñasco and Bahia Kino, consistent with the stronger gulf surge wind profiler signatures at these sites (Figs. 4a and 5a). The weaker signal at Yuma is because gulf surge intensity weakens as it fans out over the low deserts of Arizona (Hales 1972; Brenner 1974). Moderate positive moisture flux occurred at Los Mochis from 1200 UTC 12 July to 1200 UTC 13 July, but unlike the sites farther north, the strongest cooling was elevated (near 700 hPa) as was the case at R/V *Altair*. The latter results cannot be generalized because the maximum cooling at Los Mochis for the surge on 22–24 July occurred nearer the surface (not shown). The elevated cooling signal (also visible at Empalme around 1200 UTC 13 July) may be associated with evaporatively cooled air from the SMO and/or the northward advection of cooler air around TS Blas.

As TS Blas propagated northwest (Figs. 2a and 3), cooling and positive moisture flux were seen from Empalme northward by 1200 UTC 14 July as a separate feature from that of the initial gulf surge a day prior. Accompanied by moderate positive moisture flux at this time (>+50 m g s^{-1} kg^{-1}), strong cooling (−2 to −6 K) up to 700 hPa was observed. The positive moisture fluxes are explained by the strong south-southeasterly flow on 14 July, visible in the profiler data at the northern ISS sites (Figs. 4a and 5a).

Because the gulf surge vertical structure is not well defined along the southern GOC from the above methods, an along-gulf cross section (23°N, 108°W–32°N, 115°W; Fig. 1) showing the along-gulf component wind, mixing ratios, and potential temperatures was generated from the T1A gridded dataset every 6 h from 1800 UTC 12 July to 1800 UTC 13 July (Fig. 9). The cross section is influenced most by GOC coastal sounding stations, with a greater number of stations (on both sides of its axis) in the south than in the north (Fig. 1).

At 1800 UTC 12 July, moderate along-gulf flow (up to 6 m s^{-1}) was present south of 25°N from 1000 to 700 hPa. A cold-air dome had emerged along the southern GOC primarily below 800 hPa, as evident in the sloping isentropes. This feature may have been associated with a convective outflow from a large MCS that developed to the south of the GOC on 12 July (Fig. 3a). A second area of low-level cool air was observed over the central gulf, coincident with maximum mixing ratio values between 16 and 18 g kg^{-1}. Strong thunderstorms in this region earlier in the day (not shown) help explain this secondary signal. At 0000 UTC, the strongest wind was still along the southern gulf, but now above 900 hPa. The greatest moisture (>12 g kg^{-1}) was within 100 hPa of the surface and extended north to ~30°N. Given the close proximity of the large convective cloud mass near the mouth of the GOC in conjunction with TS Blas at this time (Fig. 3b), the cold air is best explained by evaporational processes although the cooling may have been enhanced by flow from the cooler waters of the eastern Pacific (Johnson et al. 2007).

The cold-air dome surged northward over the following 6 h. By 0600 UTC, a stable layer had developed below 900 hPa along the northern GOC, as evident in the tightly packed isentropes, likely aided by nocturnal cooling aliased from coastal sites out over the water. The strongest along-gulf flow was still to the south, although there was amplification of the wind below 900 hPa throughout much of the gulf. Mixing ratios less than 12 g kg^{-1} encompassed most regions to the north.

Significant changes occurred by 1200 UTC. The gulf surge reached the low deserts of northwest Mexico as the coldest air, denoted by the 302-K isentrope, now extended along the full length of the GOC. The low-level stable layer was lifted somewhat, although this feature is not well resolved by the analysis. Strong winds (>10 m s^{-1}) and abundant moisture (>16 g kg^{-1}) below 900 hPa were now over the northern gulf. These patterns qualitatively held through 1800 UTC, although the moisture maximum and winds weakened slightly over the northern gulf.

c. *Horizontal structure*

The horizontal extent of the gulf surge is more difficult to resolve than the vertical because of the spacing of rawinsonde sites around the GOC. In particular,

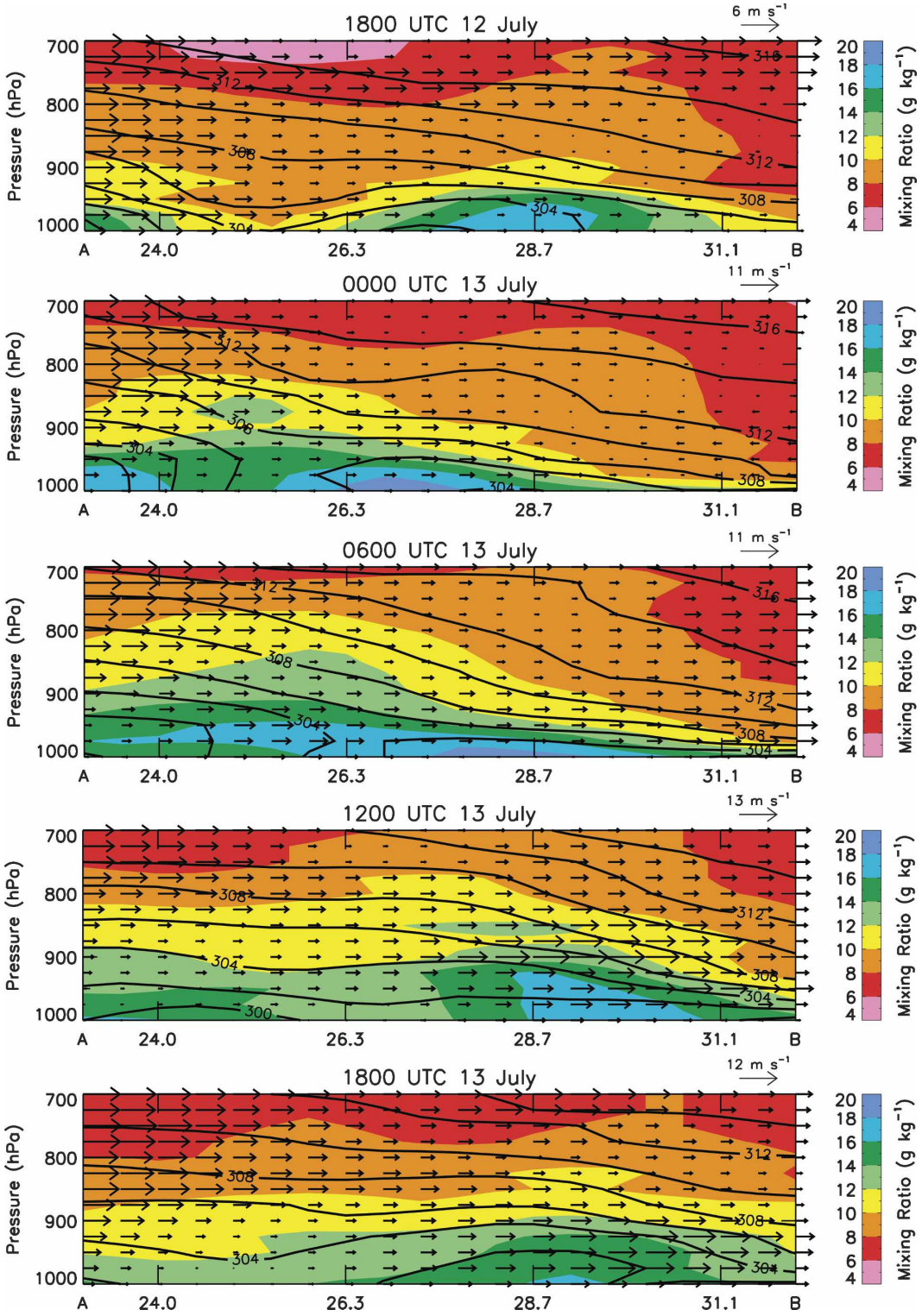

FIG. 9. T1A potential temperatures (2-K intervals), mixing ratios (g kg^{-1}), and along-gulf wind component (m s^{-1}) from 1800 UTC 12 Jul to 1800 UTC 13 Jul every 6 h along a cross section through the GOC (see Fig. 1) from 23°N, 108°W to 32°N, 115°W.

there were no upper-air observations along northern Baja California or over the northern/central GOC waters (Fig. 1). Pilot balloon observations were made along Baja California during the NAME field campaign, but were not available for this analysis. In an attempt to define the horizontal extent, gridded data from the T1A domain were used to generate 925-hPa maps from 1800 UTC 12 July to 0000 UTC 14 July showing potential temperature and moisture flux anomalies (Fig. 10). The process used to calculate the anomalies was the same as that used for Fig. 8. The 925-hPa level was used because this was the approximate averaged pressure level where gulf surge cooling and positive moisture flux appeared strongest along the northern gulf (Fig. 8).

At 1800 UTC 12 July, the region surrounding the GOC was warm, with little evidence of a gulf surge. Moderate cooling (0 to −3 K) occurred along the coastal plain by 0000 UTC 13 July centered near Los Mochis, and the beginnings of the gulf surge emerged near the mouth of the gulf, as evident in the positive moisture flux maximum. This maximum strengthened and expanded so that by 0600 UTC, it was centered slightly farther north and accompanied by cooling (−0.5 to −3 K) that encompassed the southern third of the GOC.

Six hours later (1200 UTC) the surge had reached the northern gulf. Strong cooling (−1.5 to −5 K) and positive moisture fluxes ($>+100$ m g s^{-1} kg^{-1}) were centered about Bahia Kino. Although the most prominent surge signatures were nearer the east GOC coast, this result may be biased by the locations of the rawinsonde sites along the northern gulf (Fig. 1). In fact, NOAA WP-3D measurements along the northern GOC at ~1700 UTC 13 July suggest the greatest gulf surge–related moisture flux was located over the waters of the GOC below 900 hPa and not necessarily along the gulf's eastern shores (Higgins et al. 2006). The surge signatures earlier in the day centered over the southern waters of the GOC reflect better data coverage in this region.

At 1800 UTC, the surge was confined to the northern gulf between Bahia Kino and Puerto Peñasco with strong cooling and positive moisture fluxes—a feature clearly detached from a similar signature entering the southern gulf in association with TS Blas. As the gulf surge waned by 0000 UTC 14 July along the northern gulf, the northwestward propagation of TS Blas was evident to the south. Although the results here show that the surge was primarily confined to the GOC and its eastern coastal plain, future analyses of high-resolution observations and/or mesoscale model runs must be conducted to verify this result.

5. Propagation characteristics and dynamical mechanisms

Theories for gulf surges suggest they are either advective (gravity current, isallobaric flow) or propagating (Kelvin or Rossby wave) phenomena (Zehnder 2004). The complexity of flows associated with the 13–14 July surge as well as limitations in the NAME observational network precludes a thorough analysis of surge dynamics. However, the bulk of evidence does suggest that this particular surge event was a propagating phenomenon. To determine its propagation characteristics, signatures of the profiler wind and surface pressure fields from time series at the ISS sites are examined.

In Figs. 11a–c, ISS profiler and surface winds are plotted every hour from 1800 UTC 12 July to 0000 UTC 14 July up to 2.0 km along with potential temperature anomalies (top panels), as well as 1-min resolution surface pressure and temperature anomalies (bottom panels). The anomalies presented here were calculated in the same manner as those shown in Figs. 8 and 10 such that tidal effects have been removed in a mean sense.

Prior to the surge arrival at Puerto Peñasco, two convective outflows passed this site. The first occurred shortly after 0000 UTC 13 July and the second at ~0400 UTC (Fig. 11a). Both outflows originated from convection east of Puerto Peñasco (Fig. 3b) and hence, were composed of strong (up to 8 m s^{-1}) easterly component flow. Anomalous surface pressure rises (~2–3 hPa) accompanied both features and a sharp anomalous temperature fall (~2°C) followed the outflow near 0000 UTC. The surface temperature changed little during the second outflow; as it did not appear to penetrate the very shallow stable layer near the surface (see Fig. 12). The peak winds in the surge were at a higher level (~750 m) than the convective outflows, which at this and other times during the NAME were observed to be between 300 and 500 m. Outflows are gravity current–driven phenomena and are expected to occur over a shallow layer (Wakimoto 1982).

From Fig. 11, the wind speed maxima associated with the initial gulf surge occurred at approximately 0300 UTC 13 July at Los Mochis (Fig. 11c), 1000 UTC at Bahia Kino (Fig. 11b), and 1400 UTC at Puerto Peñasco (Fig. 11a). Assuming this wind disturbance was channeled along the axis of the gulf, propagation speeds of ~17 m s^{-1} between Los Mochis and Bahia Kino and ~22 m s^{-1} between Bahia Kino and Puerto Peñasco are inferred. Another traceable feature associated with this surge event is a prolonged surface pressure rise accompanying the wind increases aloft. The onset of the pressure rise ranges from 0000 UTC 13 July

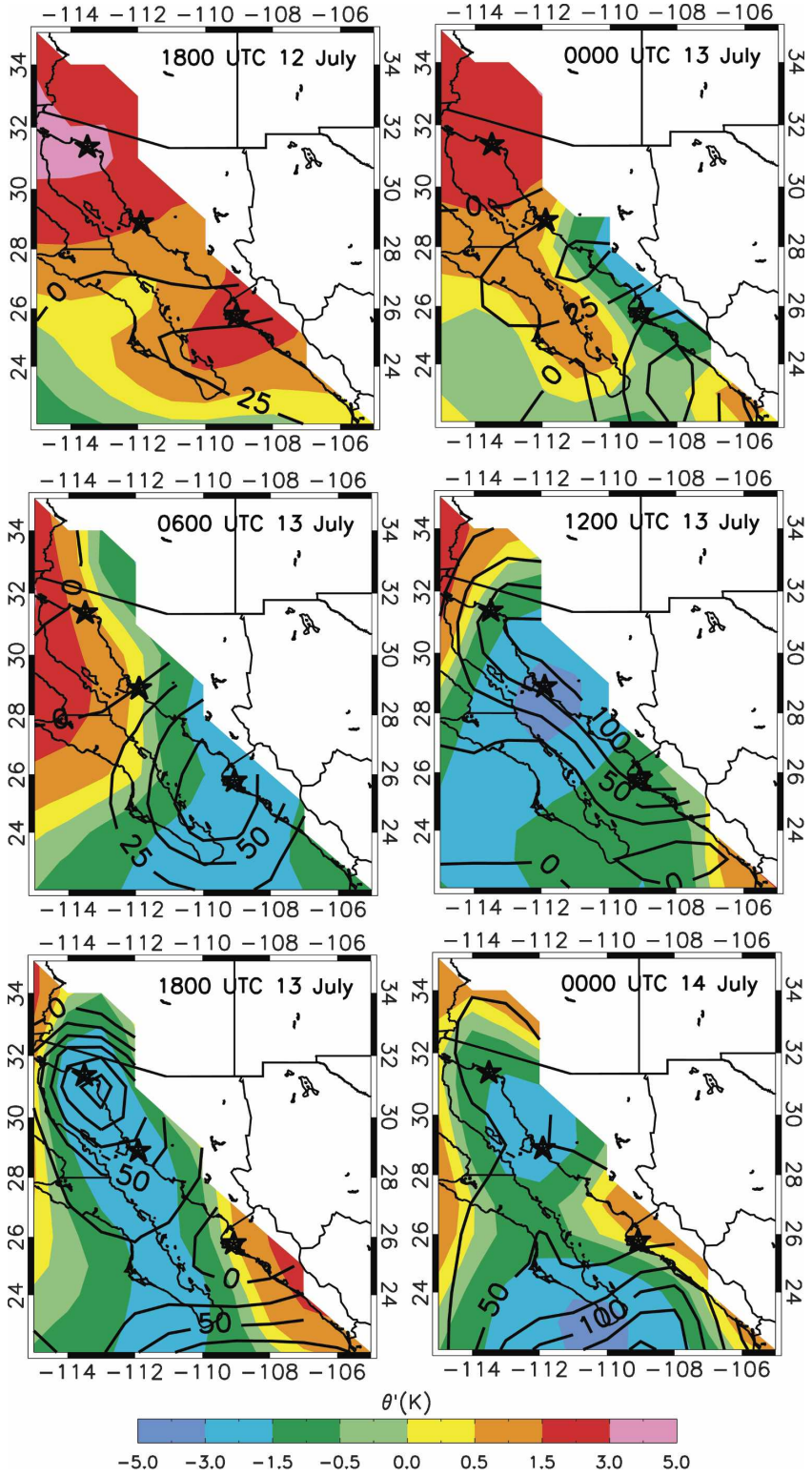

FIG. 10. T1A 925-hPa potential temperature and moisture flux anomalies from 1800 UTC 12 Jul to 0000 UTC 14 Jul 2004 every 6 h. Anomalies are calculated using 7 Jul–15 Aug means. Colored contours represent potential temperature anomalies (K). Black curves represent positive moisture flux anomalies in 25 m g s^{-1} kg^{-1} intervals. White areas are below the surface and the ISS sites are denoted by stars.

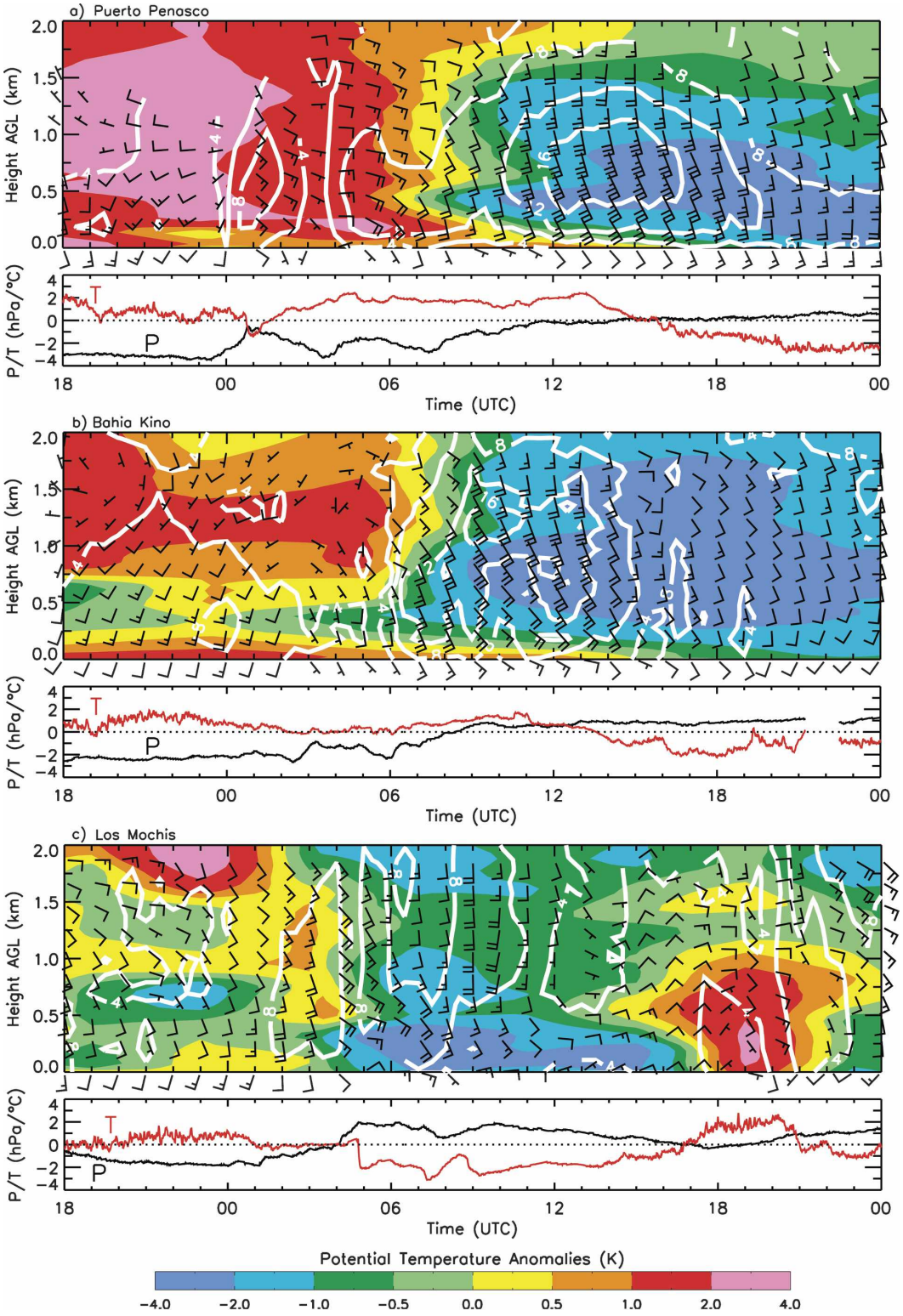

FIG. 11. (top) Half-hour interpolated rawinsonde potential temperature anomalies (K) (colored) at (a) Puerto Peñasco, (b) Bahia Kino, and (c) Los Mochis from 1800 UTC 12 Jul to 0000 UTC 14 Jul 2004. Also shown are profiler and surface wind data every hour. One full barb equals 5 m s^{-1} and the white contours highlight wind speed (m s^{-1}). (bottom) Surface pressure (hPa, black) and temperature (°C, red) anomalies every minute. See text for further details.

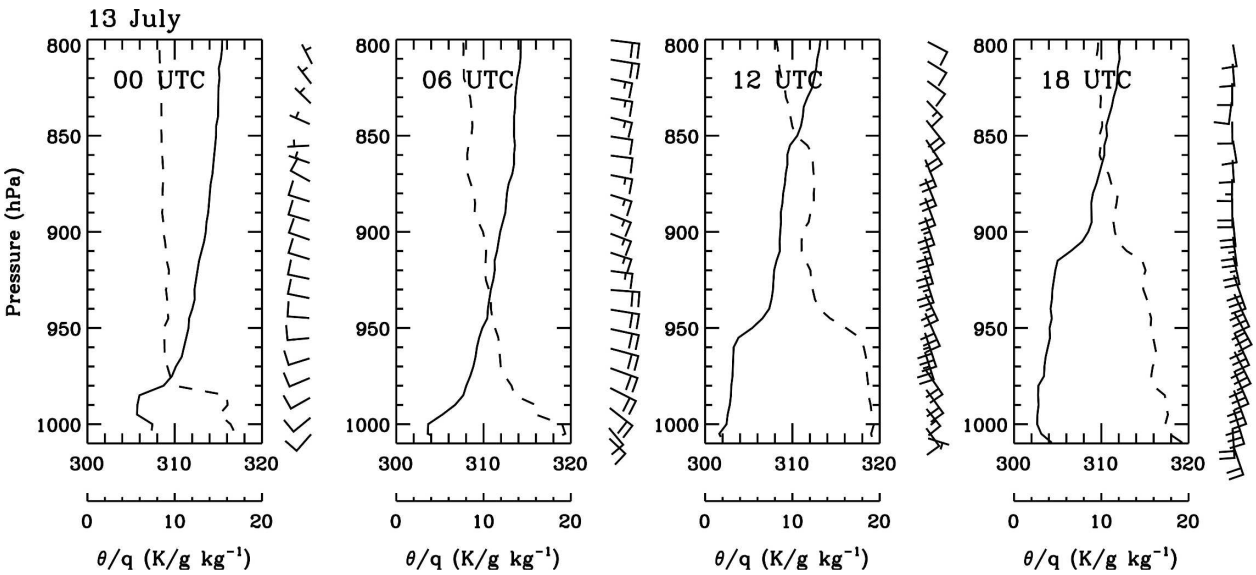

FIG. 12. Puerto Peñasco rawinsonde potential temperature (solid line, K), specific humidity (dashed line, g kg^{-1}), and wind (1 full barb = 5 m s^{-1}) profiles at 0000, 0600, 1200, and 1800 UTC 13 Jul.

at Los Mochis to approximately 0800 UTC at Puerto Peñasco, yielding an approximate 25 m s^{-1} propagation speed along the gulf. The speeds from either of these estimates exceed most of the flow speeds in the lower troposphere throughout the period, suggesting that the surge is indeed a propagating phenomenon.

The cold-air intrusion depicted in Figs. 9 and 10 originating in the south late on 12 July may have been associated with evaporational cooling from deep convection south of the mouth of the GOC (Fig. 3), possibly aided by the flow of cool air from the eastern Pacific (Johnson et al. 2007). These findings suggest that the gulf surge may have first initiated as a barrier-induced linear Kelvin wave–like disturbance (Reason and Steyn 1992; Skamarock et al. 1999; Zehnder 2004). However, the calculated gulf surge propagation speed (~17–25 m s^{-1}) is too fast for a linear Kelvin wave (~10–15 m s^{-1}; Ralph et al. 2000). Speeds of ~20 m s^{-1} seem to fall more in line with nonlinear wave phenomena, such as atmospheric bores (Simpson 1997), which have been found to propagate at speeds greater than 15 m s^{-1} across portions of Oklahoma (Fulton et al. 1990) and the mid-Atlantic states (Koch et al. 1991). There is also the possibility that the surge behaves like a mixed Kelvin wave bore, as has been found for coastally trapped wind reversals along the California coast (Ralph et al. 2000).

Bores are generally shallow-water disturbances that propagate along the tops of low-level stable layers and resemble a hydraulic jump, in which fluid depth significantly increases after passage (Simpson 1997). The fact that the surge arrived during the nighttime hours (particularly over the northern gulf) following the development of a nocturnal inversion over the coastal plain raises the possibility that at least the initial surge impulse resembled a borelike disturbance.

Boundary layer observations at Puerto Peñasco (Fig. 12) indicate low-level inversions at 0000 and 0600 UTC 13 July. Downdraft outflows from convection (Fig. 3) impinging on this low-level stable layer would be capable of lifting it and creating a bore. In fact, the multiple convective systems in the region (Fig. 3) may have contributed to several bores over the area, much as has been observed at night during the International H_2O Project (Weckwerth et al. 2004). Low-level stable layers over land are associated with nocturnal inversions; over water, low-level inversions are also frequently observed (inferred from the coastal Puerto Peñasco site during onshore southerly flow) as a result of marine air overlain by hot, desert air. The shelflike layer of cooling just below 500 m at Bahia Kino and Puerto Peñasco in Fig. 11 may be evidence of bore-related cooling.

Further evidence of borelike behavior is the rapid rise of the surface pressure to a new level, especially at Puerto Peñasco (Fig. 11a) and Bahia Kino (Fig. 11b), which is a characteristic feature of bores (Simpson 1997). Following this initial impulse there is a deeper layer of cooling that extends to the surface and strong (up to 20 m s^{-1}) south-southeasterly wind, which may be related to a Kelvin wave. The Puerto Peñasco potential temperature and specific humidity profiles at

1200 and 1800 UTC (Fig. 12) indicate a deepening mixed layer accompanying this feature as the strong wind and turbulence extend the boundary layer upward. Another indication of a borelike disturbance is the fact that the surface temperatures at Puerto Peñasco and Bahia Kino (Figs. 11a,b) did not immediately fall with passage of the disturbance. Instead, they rose slightly and only fell later with the presumed Kelvin wave disturbance. The slight warming may have been a result of downward mixing of warmer air at night and/or temporary horizontal advection of warmer air from the GOC.

Surge-related features similar to those at Puerto Peñasco and Bahia Kino are not as evident at Los Mochis (Fig. 11c). The strong cooling (−1 to −4 K) below 500 m from 0400 to 1600 UTC 13 July is related to an intense convective outflow that passed the site between 0400 and 0500 UTC. The outflow originated from the westward-propagating convection off the SMO (Figs. 3b,c), was dominated by easterly component flow, and resulted in a coincident strong anomalous surface pressure (temperature) rise (fall). The coincident moderate cooling (−1 to −2 K) and south-southeasterly flow (up to 10 m s^{-1}) from 500 m up to 2.0 km is a response to surge passage. This overall surge signature did not last long and was interrupted around 1800 UTC by strong warming and an increased easterly component flow aloft, thus highlighting the importance of local effects and Los Mochis's more inland location.

The sequence of events occurring on 13–14 July is complex and subject to several possible interpretations. However, the weight of the evidence presented here suggests that the initial surge over the northern gulf resembles borelike disturbances that owed their existence to convective downdrafts impinging on the low-level stable layer over the region. Strong pressure rises to a new level accompanied the passage of these disturbances at Bahia Kino and Puerto Peñasco. Following these initial pulses, a deeper layer of sharp cooling and strong wind ensued, which likely represents a Kelvin wave that traveled along the entire gulf. Pressures continued to rise as this feature passed. Another possibility is that the leading edge of this Kelvin wave steepened nonlinearly into a borelike disturbance (Skamarock et al. 1999). The data are not adequate to delineate between these possible mechanisms.

6. Summary and conclusions

Gulf surges are complex atmospheric phenomena, yet extremely important to the NAM as they are often associated with northward horizontal transport of cool, moist air to the low deserts of the southwest United States and northwest Mexico, at times resulting in explosive convective development over this region. This study reports on high-resolution wind profiler, rawinsonde, and surface observations of a prominent gulf surge on 13–14 July during the 2004 NAME. The surge structure and properties have been defined in a detail heretofore not possible.

The 13–14 July gulf surge was strong and deep (up to ~800 hPa), resulting in increased convective development over southern Arizona. The initial surge quickly traversed the length of the GOC at speeds of approximately 17–25 m s^{-1}. However, it was stronger and shallower in the north than the south, perhaps due to its arrival in the north at the time of the GOC LLJ. TS Blas propagated northwestward from south of the mouth of the GOC to the open waters of the eastern Pacific Ocean during the gulf surge event. The tropical cyclone, in conjunction with the convection that developed along the SMO and GOC coastal plain after 0000 UTC 13 July, played an integral role in gulf surge initiation due to strong evaporational cooling over the region.

Preceded by anomalous warming (+2 to +6 K) and a low-level stable layer along the northern GOC coastal plain, the surge was first observed near the mouth of the gulf as a large low-level cold dome. As the disturbance moved north, a strong increase in south-southeasterly flow (up to 20 m s^{-1} near 750 m at Puerto Peñasco and 1.25 km at Bahia Kino), anomalous cooling (−1 to −4 K), and anomalous positive moisture flux (>+150 m g s^{-1} kg^{-1}) were observed along the northern gulf. These patterns lasted approximately 12–18 h, followed by a brief break and then a strong resurgence of anomalous cooling and southerly flow over a deeper layer associated with the passage of TS Blas on 14 July. Surface signals related to surge passage included substantial increases in surface pressure, initial surface warming followed by moderate cooling, and a moderate strengthening of the wind from the south-southeast. These characteristics were more difficult to discern along the southern gulf.

The horizontal extent of the gulf surge was difficult to resolve because of the few rawinsonde sites along the GOC coasts, especially in the north and along Baja California. Nevertheless, surge strength appeared to be greatest near the waters of the GOC and confined to the natural channel created by the surrounding terrain.

Inferences regarding the dynamics of the gulf surge are inconclusive, but the data suggest that the early stage of the surge consisted of two parts. First, the surge likely originated from cooling by convective downdrafts impinging on the low-level nocturnal and marine inver-

sions over the coastal region, advancing initially as a series of bores (particularly in the north), and was amplified by the nocturnal LLJ in the north. Second, a Kelvin wave disturbance followed that propagated the length of the GOC. The leading edge of this Kelvin wave may have steepened nonlinearly into a borelike disturbance, but this possibility cannot be resolved by the data. These features were accompanied by strong surface pressure rises to a new level and a deepening of the mixed layer along the northern gulf.

The results presented here reveal the complexity of the 13–14 July gulf surge and the environment in which it propagated. It is uncertain whether the observations can be applied in part or in whole to other gulf surge events. Future work should focus on further integrating other observational platforms from the 2004 NAME field campaign (i.e., aircraft, pilot balloon, radar, precipitation, etc.) into the gridded analyses as a means to more accurately compare against mesoscale model simulations. Only then can a more complete picture emerge concerning gulf surge structure and probable dynamical mechanisms.

Acknowledgments. This research has been supported by the National Science Foundation Mesoscale Dynamic Meteorology Program under Grant ATM-0340602, the National Oceanic and Atmospheric Administration Office of Global Programs under Grant NA17RJ1228, and a 1-yr American Meteorological Society Graduate Fellowship. Special thanks to Paul Ciesielski and Brian McNoldy are also in order for their assistance throughout this project. The comments of Bob Maddox and an anonymous reviewer led to considerable improvements in the manuscript.

REFERENCES

Adams, D. K., and A. C. Comrie, 1997: The North American Monsoon. *Bull. Amer. Meteor. Soc.,* **78,** 2197–2213.

Brenner, I. S., 1974: A surge of maritime tropical air—Gulf of California to the southwestern United States. *Mon. Wea. Rev.,* **102,** 375–389.

Bryson, R. A., and W. P. Lowry, 1955: Synoptic climatology of the Arizona summer precipitation singularity. *Bull. Amer. Meteor. Soc.,* **36,** 329–339.

Douglas, M. W., 1995: The summertime low-level jet over the Gulf of California. *Mon. Wea. Rev.,* **123,** 2334–2347.

——, and S. Li, 1996: Diurnal variation of the lower-tropospheric flow over the Arizona low desert from SWAMP-1993 observations. *Mon. Wea. Rev.,* **124,** 1211–1224.

——, and J. C. Leal, 2003: Summertime surges over the Gulf of California: Aspects of their climatology, mean structure, and evolution from radiosonde, NCEP reanalysis, and rainfall data. *Wea. Forecasting,* **18,** 55–74.

——, R. A. Maddox, K. Howard, and S. Reyes, 1993: The Mexican monsoon. *J. Climate,* **6,** 1665–1677.

——, A. Valdez-Mananilla, and R. G. Cueto, 1998: Diurnal variation and horizontal extent of the low-level jet over the northern Gulf of California. *Mon. Wea. Rev.,* **126,** 2017–2025.

Fuller, R. D., and D. J. Stensrud, 2000: The relationship between tropical easterly waves and surges over the Gulf of California during the North American Monsoon. *Mon. Wea. Rev.,* **128,** 2983–2989.

Fulton, R., D. S. Zrnić, and R. J. Doviak, 1990: Initiation of a solitary wave family in the demise of a nocturnal thunderstorm density current. *J. Atmos. Sci.,* **47,** 319–337.

Hales, J. E., Jr., 1972: Surges of maritime tropical air northward over the Gulf of California. *Mon. Wea. Rev.,* **100,** 298–306.

Higgins, R. W., and W. Shi, 2005: Relationships between Gulf of California moisture surges and tropical cyclones in the eastern Pacific basin. *J. Climate,* **18,** 4601–4620.

——, ——, and C. Hain, 2004: Relationships between Gulf of California moisture surges and precipitation in the southwestern United States. *J. Climate,* **17,** 2983–2997.

——, and Coauthors, 2006: The NAME 2004 field campaign and modeling strategy. *Bull. Amer. Meteor. Soc.,* **87,** 79–94.

Johnson, R. H., P. E. Ciesielski, B. D. McNoldy, P. J. Rogers, and R. K. Taft, 2007: Multiscale variability of the flow during the North American Monsoon Experiment. *J. Climate,* **20,** 1628–1648.

Jurwitz, L. R., 1953: Arizona's two-season rainfall pattern. *Weatherwise,* **6,** 96–99.

Kalnay, E., and Coauthors, 1996: The NCEP/NCAR 40-Year Reanalysis Project. *Bull. Amer. Meteor. Soc.,* **77,** 437–471.

Koch, S. E., P. B. Dorian, R. Ferrare, S. H. Melfi, W. C. Skillman, and D. Whiteman, 1991: Structure of an internal bore and dissipating gravity current as revealed by raman lidar. *Mon. Wea. Rev.,* **119,** 857–887.

Loehrer, S. M., T. A. Edmands, and J. A. Moore, 1996: TOGA COARE upper-air sounding data archive: Development and quality control procedures. *Bull. Amer. Meteor. Soc.,* **77,** 2651–2671.

McCollum, D. M., R. A. Maddox, and K. W. Howard, 1995: Case study of severe mesoscale convective system in central Arizona. *Wea. Forecasting,* **10,** 643–665.

Nuss, W. A., and D. W. Titley, 1994: Use of multiquadric interpolation for meteorological objective analysis. *Mon. Wea. Rev.,* **122,** 1611–1631.

Pytlak, E., M. Goering, and A. Bennett, 2005: Upper tropospheric troughs and their interaction with the North American Monsoon. Preprints, *19th Conf. on Hydrology,* San Diego, CA, Amer. Meteor. Soc., CD-ROM, JP2.3.

Ralph, F. M., P. J. Neiman, P. O. G. Persson, J. M. Bane, M. L. Cancillo, J. M. Wilczak, and W. Nuss, 2000: Kelvin waves and internal bores in the marine boundary layer inversion and the relationship to coastally trapped wind reversals. *Mon. Wea. Rev.,* **128,** 283–300.

Rasmusson, E. M., 1967: Atmospheric water vapor transport and the water balance of North America. *Mon. Wea. Rev.,* **95,** 403–426.

Reason, C. J. C., and D. G. Steyn, 1992: The dynamics of coastally trapped mesoscale ridges in the lower atmosphere. *J. Atmos. Sci.,* **49,** 1677–1692.

Reitan, C. H., 1957: The role of precipitable water vapor in Arizona's summer rains. Meteorology and climatology of arid regions Tech. Rep. 2, 19 pp.

Sellers, W. D., and R. H. Hill, 1974: *Arizona Climate 1931–1972.* 2d ed. The University of Arizona Press, 616 pp.

Simpson, J. E., 1997: *Gravity Currents in the Environment and the Laboratory.* 2d ed. Cambridge University Press, 244 pp.

Skamarock, W. C., R. Rotunno, and J. B. Klemp, 1999: Models of coastally trapped disturbances. *J. Atmos. Sci.,* **56,** 3349–3365.

Stensrud, D. J., R. L. Gall, and M. K. Nordquist, 1997: Surges over the Gulf of California during the Mexican monsoon. *Mon. Wea. Rev.,* **125,** 417–437.

Wakimoto, R. M., 1982: The life cycle of thunderstorm gust fronts as viewed with Doppler radar and rawinsonde data. *Mon. Wea. Rev.,* **110,** 1060–1082.

Weckwerth, T. M., and Coauthors, 2004: An overview of the International H_2O Project (IHOP_2002) and some preliminary highlights. *Bull. Amer. Meteor. Soc.,* **85,** 253–277.

Zehnder, J. A., 2004: Dynamic mechanisms of the gulf surge. *J. Geophys. Res.,* **109,** D10107, dio:10.1029/2004JD004616.